



COMPUTER-AIDED ENGINEERING (CAE) APPROACH IN THE BENDING ANALYSIS OF A COMPOSITE BEAM

Fatih Karacam*, FerudunDoğuş Yılmaz

Trakya University, Department of Mechanical Engineering, Edirne, Turkey

ARTICLE INFO

Article history:

Received 3 October 2019

Accepted 21 November 2019

Keywords:

bending analysis, composite beam, FEM

ABSTRACT

Bending analysis of a symmetric cross-ply beam subjected to a uniform distributed load with different boundary conditions is performed by utilizing finite element method through a computer aided engineering (CAE) software. In this study, 3-D modelling with brick elements is used in order to have an alternative reference solution, although modelling with conventional and continuum shell elements are appropriate choices for composite structures. The longitudinal and vertical in-plane displacements, shear and normal stresses are examined at different points and sections of the beam. The results are compared with the analytical and computational solutions available in the literature, and the in-plane displacement and bending stress distributions are illustrated for various boundary conditions.

© 2019 Journal of the Technical University of Gabrovo. All rights reserved.

INTRODUCTION

The use of composite materials in aerospace and aviation engineering applications are inevitable in today's world of science as they provide much better features, such as high specific strengths and modulus. Thus, such investigations and analysis about, in particular, beams', plates' and shells', are becoming increasingly important.

Karama et al. [4, 5] performed the static and dynamic behaviors of cross-ply beams subjected to sinusoidal and uniform distributed loading for different boundary conditions by taking into account of the transverse shear stress continuity conditions. Zhang et al. [6] investigated quasi-static four-point bending behaviors and failure characteristics of a large scale composite C-beams fastened with multi-bolt joints experimentally and numerically. Karacam and Timarci [7] performed the bending analysis of cross-ply laminated beams subjected to a uniform distributed loading for different boundary conditions, which is presented by use of a unified three-degree-of-freedom shear deformable beam theory. Meydanlik et al. [8] extended the previous study by taking into consideration the angle-ply beams with the help of a computer aided design package. Ashfaq et al. [9] studied the macro bending effects in optical fiber units of optical fiber composite low voltage cables that occurs in handling and installation process of the cables. They used a computer aided design software, analyzed and investigated the attenuation loss at different bending radiuses and number of turns. Prabhakaran et al. [10] investigated the effects of the flax fiber lay-ups and orientation to the laminated composites in bending. Unidirectional $[0^\circ]_{2S}$, cross-ply $[0^\circ/90^\circ]_S$, and angle-ply $[+45^\circ/-45^\circ]_S$ laminates made up of flax fiber

reinforced epoxy composites are considered to investigate flexural stresses and mid-span deflections.

The main objective of this study is to investigate the computer aided engineering (CAE) approach in the bending analysis of a cross-ply composite beam and to compare the results with the ones obtained by Ref. [4, 5] and Ref. [7, 8]. The bending analysis of a symmetric cross-ply $[90^\circ/0^\circ]_S$ beam subjected to a uniform distributed load with different boundary conditions, is performed by utilizing a CAE software. The results are compared with the analytical and computational solutions of the previous studies. In the software, instead of other conventional and continuum shell element methods of modeling, solid modeling with brick elements is used.

2. ANALYTICAL METHOD

In the study, the beam with a rectangular cross section, a thickness of h , length of L and unit width is considered. The coordinate system is placed at the geometric center of the left surface, the beam is assumed to be constructed of 4 linearly elastic layers under the effect of a uniform distributed transverse load ($q(x)$). U and W indicates the in-plane displacements of any section of the beam with respect to x - and z - axis, respectively. The displacement field below is assumed to be parallel with general shear deformation beam theory as presented in [2]: Where “,” denotes differentiation with respect to relevant axis, u, w and u_1 are the three unknown displacement functions of the middle surface of the beam. A parabolic shape function (ϕ), which depends on the material geometry and properties, is chosen.

* Corresponding author. E-mail: fatihkar@trakya.edu.tr

$$\begin{aligned} U(x, z) &= u(x) - zw_{,x} + \phi(z)u_1(x) \\ W(x, z) &= w(x) \end{aligned} \quad (1)$$

The kinematic relations depending on the displacement fields are given as below;

$$\begin{aligned} \varepsilon_x &= u_{,x} - zw_{,xx} + \phi'(z)u_{1,x} \\ \gamma_{xz} &= \phi'(z)u_1 \end{aligned} \quad (2)$$

The state of stresses regarding to each k^{th} layer is given in the form of Hooke's law as seen below where $Q_{ij}^{(k)}$ terms are the reduced stiffness [1].

$$\begin{bmatrix} \sigma_x^{(k)} \\ \tau_{xz}^{(k)} \end{bmatrix} = \begin{bmatrix} Q_{11}^{(k)} & 0 \\ 0 & Q_{55}^{(k)} \end{bmatrix} \begin{bmatrix} \varepsilon_x \\ \gamma_{xz} \end{bmatrix} \quad (3)$$

Use of this relation into force and moment definitions [3], the following governing equations are obtained, where A , B , D and Q_x^a represent the extensional, coupling, bending rigidities and shear force respectively.

$$\begin{bmatrix} N_x^k \\ M_x^k \\ M_x^a \end{bmatrix} = \begin{bmatrix} A_{11} & B_{11} & B_{111} \\ B_{11} & D_{11} & D_{111} \\ B_{111} & D_{111} & D_{1111} \end{bmatrix} \begin{bmatrix} u_{,x} \\ -w_{,xx} \\ u_{1,x} \end{bmatrix} \quad (4)$$

$$Q_x^a = A_{55}u_1$$

The governing equations of a rectangular cross-sectional beam can be obtained by use of virtual work principle as follows:

$$\begin{aligned} N_{x,x} &= 0 \\ M_{x,xx} &= q(x) \\ M_{x,x}^a - Q_x^a &= 0 \end{aligned} \quad (5)$$

The use of comprehensive equations (4) in the equations (5) leads to the following the set of differential equations containing the three unknown functions and their derivatives with respect to axial coordinate of the beam:

$$\begin{aligned} A_{11}u_{,xx} - B_{11}w_{,xxx} + B_{111}u_{1,xx} &= 0 \\ B_{11}u_{,xxx} - D_{11}w_{,xxxx} + D_{111}u_{1,xxx} &= q(x) \\ B_{111}u_{,xx} - D_{111}w_{,xxx} + D_{1111}u_{1,xx} - A_{55}u_1 &= 0 \end{aligned} \quad (6)$$

Restrictions for the simply supported, clamped and free boundary conditions are given in the following way respectively:

$$\begin{aligned} N_x = w = M_x = M_x^a &= 0 \\ u = w = w_{,x} = u_1 &= 0 \\ N_x = M_{x,x} = M_x = M_x^a &= 0 \end{aligned} \quad (7)$$

3. COMPUTATIONAL METHOD

In this study, Abaqus CAE 2017 Student Edition is utilized for the computational solution, which is a finite element analysis software for computer aided engineering. 3-D brick elements are chosen as the method of solid modeling. The plane and shell elements are generally considered as acceptable and effective enough to model and analyze composite laminates since they yield adequate

amount of accuracy. On the other hand, since 3-D modeling is a more realistic approach to this structural problem, numerical results are expected to be more precise. The shape and type of the element are chosen as solid and extrusion. After cutting the element into 4 layers with partition cell option, material properties that are taken from [7] are inserted. After the properties are assigned to each layer individually, the coordinate system, which will be used for defining fiber orientation, is established. Through this coordinate system, orientation of the fibers are acquired as $[90^\circ/0^\circ]_S$. After the loading type and boundary conditions are defined, meshing is made in a way that there would be 4 rows of finite elements for each layer.

4. NUMERICAL RESULTS

In the study, the beam is assumed to be constructed of graphite/epoxy layers with a length of $L = 6.35\text{ m}$, thickness of $h = 2.794\text{ mm}$ and under a uniform transverse distributed load of $q_0 = 1000\text{ N/m}$. Material properties used in the analysis are given below;

$$\begin{aligned} E_{11} &= 241.5\text{ GPa}, E_{22} = E_{33} = 18.8\text{ GPa}, \\ G_{23} &= 3.45\text{ GPa}, G_{12} = G_{13} = 5.18\text{ GPa}, \\ \nu_{23} &= 0.25, \nu_{12} = \nu_{13} = 0.24. \end{aligned}$$

In Table 1 and Table 2, the in-plane displacements, bending stresses and error (%) are presented for different boundary conditions. The percentages of errors are calculated through the formula below;

$$Error(\%) = \left(\frac{Ref. - Study}{Ref.} \right) \times 100 \quad (8)$$

Except for τ_{xz} , which has the biggest percentage of error, this study has the closest numerical results to the abaqus CAE solution in Ref. 4. The differences between the results might occur due to the formulations that CAE software uses in 2-D and 3-D analysis, the choices of the element types, mesh numbers and the degrees of correlations of the mesh elements. It is obvious from Table 2 that, when compared with Ref. 7, even though the differences between longitudinal displacement and shear stress are relatively small, the ones between vertical displacements and normal stresses are quiet significant.

In Fig. 1-3-5, the normal stress (σ_{xx}), in Fig. 2-4-6, the shear stress (τ_{xz}) distributions are presented for C-C, C-F and S-S boundary conditions respectively. In Fig. 7-9-11, the in-plane displacement (U) and in Fig. 8-10-12, the in-plane displacement (W) are presented for the same combination of boundary conditions. The normal stresses and vertical in-plane displacements are obtained along the beam length, where the shear stresses and longitudinal in-plane displacements are obtained along the beam thickness respectively.

Table 1. In-plane displacements and bending stresses for C-F case

Model	$\sigma_{xx}(L/2, -h/4)$ (Pa)	$\tau_{xz}(L/4, 0)$ (Pa)	$U(L/2, h/2)$ (m)	$W(L)$ (m)
This Study	-10535.60	-3233.40	$8.0827 \cdot 10^{-7}$	$-4.6186 \cdot 10^{-6}$
Error (%)	2.8	3.9	0.9	2.2
Karacam (2005)	-10173.24	-3019.43	$7.0118 \cdot 10^{-7}$	$-4.2551 \cdot 10^{-6}$
Error (%)	6.2	2.9	14.0	5.8
Karama (2003)	-9986.18	-3181.03	$7.3649 \cdot 10^{-7}$	$-4.4005 \cdot 10^{-6}$
Error (%)	7.9	2.3	9.8	2.6
Karama (1998)	-10842.00	-3110.00	$8.1630 \cdot 10^{-7}$	$-4.5181 \cdot 10^{-6}$

Table 2. In-plane displacements and bending stresses for C-C case

Model	$\sigma_{xx}(L/2, -h/4)$ (Pa)	$\tau_{xz}(L/4, 0)$ (Pa)	$U(L/4, h/2)$ (m)	$W(L/2)$ (m)
This Study	2969.74	-983.706	$9.14888 \cdot 10^{-8}$	$-5.36614 \cdot 10^{-7}$
Error (%)	8.6	1.7	0.4	10.4
Karacam (2005)	2733.07	-1000.80	$9.1118 \cdot 10^{-8}$	$-4.85849 \cdot 10^{-7}$

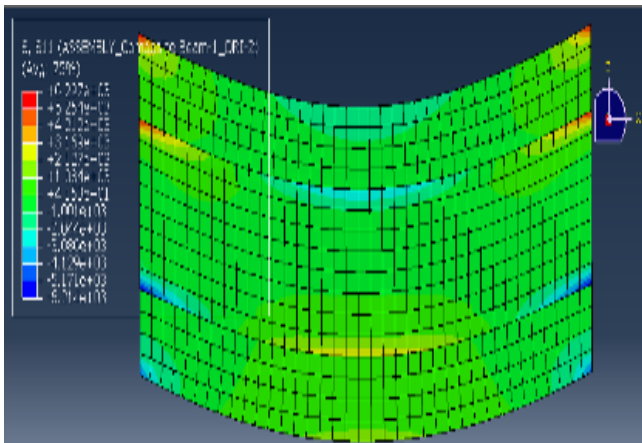


Fig. 1. Normal stress (σ_{xx}) distribution for C-C boundary condition

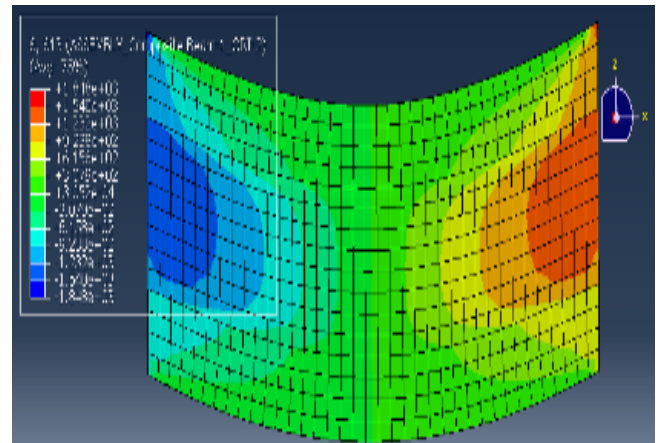


Fig. 2. Shear stress (τ_{xz}) distribution for C-C boundary condition

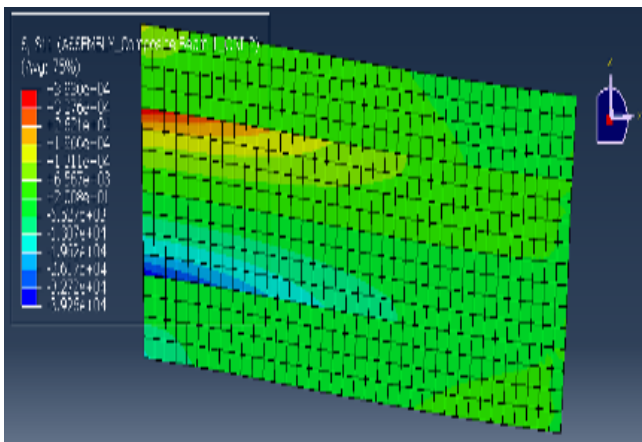


Fig. 3. Normal stress (σ_{xx}) distribution for C-F boundary condition

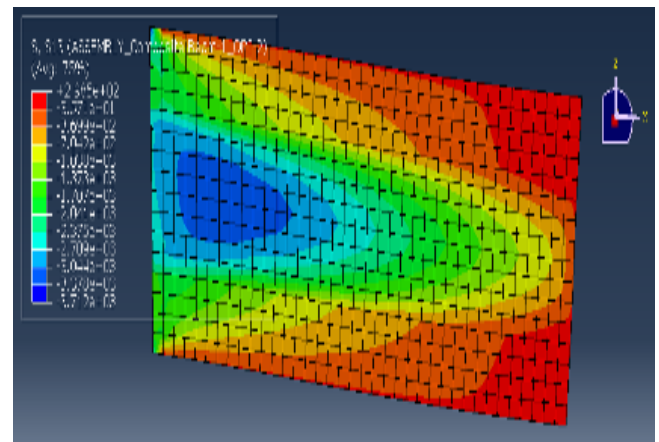


Fig. 4. Shear stress (τ_{xz}) distribution for C-F boundary condition

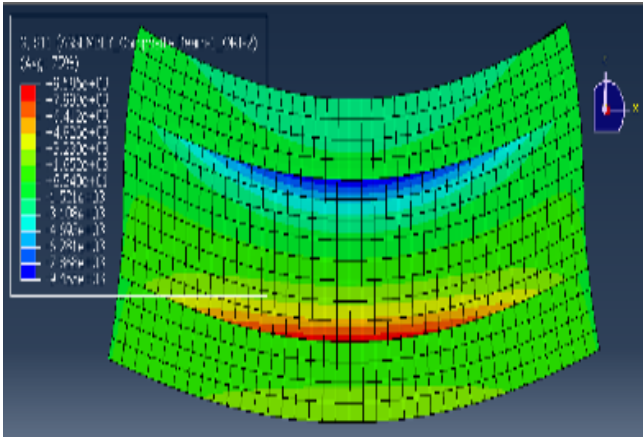


Fig. 5. Normal stress (σ_{xx}) distribution for S-S boundary condition

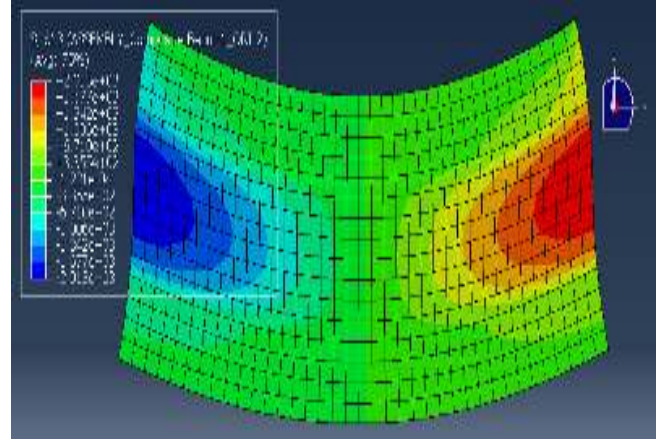


Fig. 6. Shear stress (τ_{xz}) distribution for S-S boundary condition

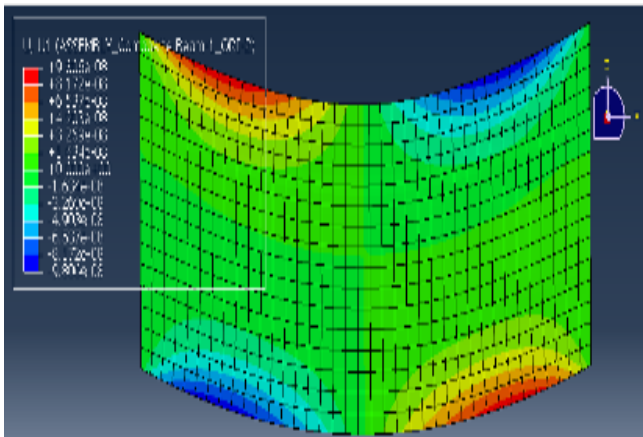


Fig. 7. In-plane displacement (U) distribution for C-C boundary condition

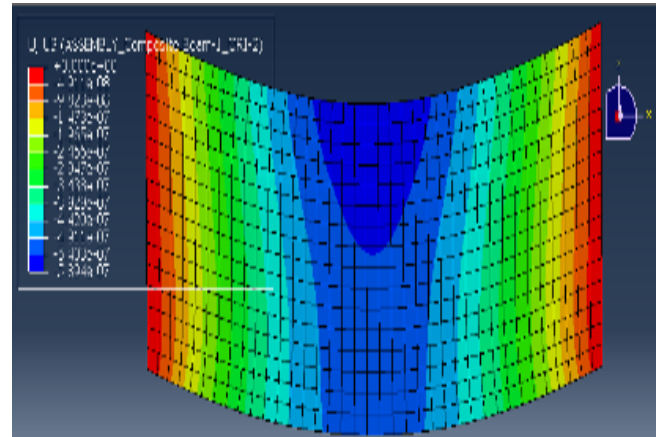


Fig. 8. In-plane displacement (W) distribution for C-C boundary condition

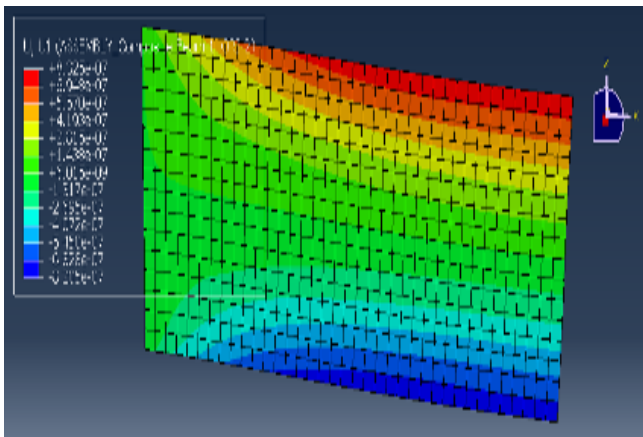


Fig. 9. In-plane displacement (U) distribution for C-F boundary condition

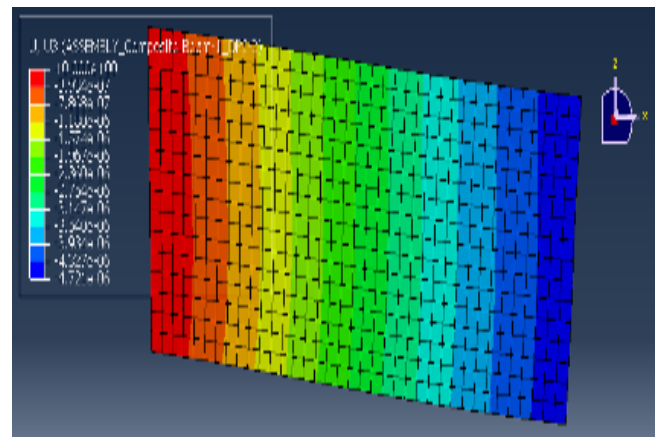


Fig. 10. In-plane displacement (W) distribution for C-F boundary condition

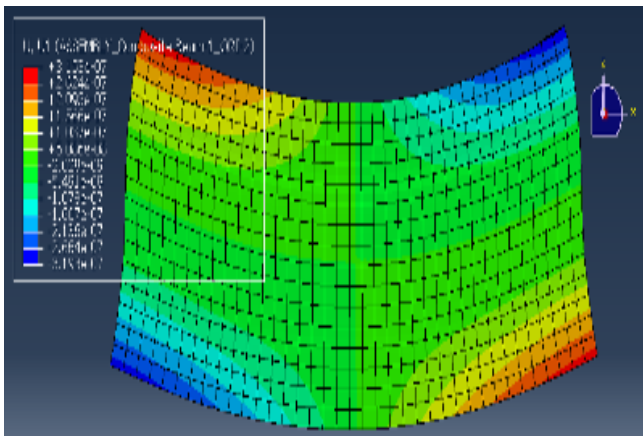


Fig. 11. In-plane displacement (U) distribution for S-S boundary condition

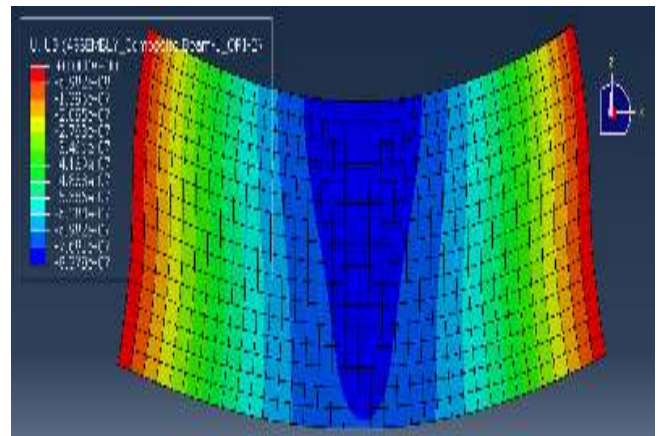


Fig. 12. In-plane displacement (W) distribution for S-S boundary condition

5. CONCLUSIONS

In the study, the governing equations of the cross-ply $[90^\circ/0^\circ]_S$ beam under a uniformly distributed load are solved analytically on the basis of a parabolic shear deformable beam theory for various boundary conditions. The results obtained are compared with the ones obtained analytically. This analytical results are visualized through curved and colored graphics. On the curved graphics, while the longitudinal displacements and shear stresses are obtained through the beam thickness, vertical displacements and normal stresses are obtained along the length of beam. To have an alternative reference solution, solid modelling with 3-D brick elements is utilized in the software.

The study gives the most accurate results, except for the shear stress for C-F case when compared with the reference. For C-C case, the biggest difference on vertical displacements is at $L/2$, while the horizontal displacements and shear stresses don't show any significant disparity with the analytical solution.

The study can be extended with various stacking sequences, number of layers, material and geometrical properties, and boundary conditions. For a further work, the dynamic analyses including the fundamental natural frequencies and critical buckling loads for different boundary conditions can be investigated.

REFERENCES

- [1] Jones R. M., Mechanics of composite materials. New York: McGraw-Hill, 1975.
- [2] Soldatos K. P., Timarci T., A unified formulation of laminated composite, shear deformable five-degrees-of freedom cylindrical shell theories. Composite Structures, 1993; 25: 165-171.
- [3] Timarci T., Soldatos K. P., Comparative dynamic studies for symmetric cross-ply circular cylindrical shells on the basis of a unified shear deformable shell theory. Journal of Sound and Vibration, 1995; 187(4): 609-624.
- [4] Karama M., Harb B. A., Mistou S., Caperaa S., Bending, buckling and free vibration of laminated composite with a transverse shear stress continuity model. Composites Part B, 1998; 29 (B): 223-234.
- [5] Karama M., Afaq K. S., Mistou S., Mechanical behaviour of laminated composite beam by the new multi-layered laminated composite structures model with transverse shear stress continuity. International Journal of Solids and Structures, 2003; 40: 1525-1546.
- [6] Zhang F., Zhang W., Hu Z., Jin L., Jia X., Wu L., Wan Y., Experimental and numerical analysis of the mechanical behaviors of large scale composite C-beams fastened with multi-bolt joints under four-point bending load. Composites Part B, 2019; 164: 168-178.
- [7] Karacam F., Timarci T., Bending of cross-ply beams with different boundary conditions. In: UNITECH Gabrovo-05 Proceedings, International Scientific Conference, vol. II, 2005, p. 137-142.
- [8] Meydanlık N., Karacam F., Timarci T., Bending analysis of laminated composite beams by use of a finite element method package. In: UNITECH Gabrovo-07 Proceedings, International Scientific Conference, vol. II, 2007, p. 132-136.
- [9] Ashfaq A., Chen Y., Yao K., Sun G., Yu J., Macro bending effect in optical fiber composite low voltage cable. In: Proceedings of IEEE 2nd International Conference on Dielectrics (ICD), 2018.
- [10] Prabhakaran R. T. D., Ormondroyd G. A., Zhongwei G., Flax/Epoxy composite beams - simulation of flexural stresses. In: Materials Today Proceedings, vol. VIII, 2019, p. 760-768.